The single-layer/bilayer transition of electron systems in AlGaAs/GaAs/AlGaAs quantum wells subject to in-plane magnetic fields

1995 J. Phys.: Condens. Matter 7 3721

(http://iopscience.iop.org/0953-8984/7/19/006)

J. Phys.: Condens. Matter 7 (1995) 3721–3732. Printed in the UK

The single-layer/bilayer transition of electron systems in AlGaAs/GaAs/AlGaAs quantum wells subject to in-plane magnetic fields

L Smrčka and T Jungwirth

Institute of Physics, Academy of Science of the Czech Republic, Cukrovarnická 10, 162 00 Praha 6, Czech Republic

Received 9 January 1995

Abstract. Equilibrium properties of electrons in double-heterojunction AlGaAs/GaAs/AlGaAs structures are investigated theoretically, using a fully self-consistent numerical method. The transition from single to bilayer electron systems is discussed for structures with varying distance between interfaces as a function of the in-plane magnetic field strength. A phenomenon of separability of the energy dispersion curves in parts corresponding to electrons in either the first or the second layer is analysed in detail. The magnetic-field-induced variation in the effective distance between electron layers is compared to the constant layer separation in standard double-well structures. Because the barrier between interfaces is relatively small and soft, the van Hove singularities in the 2D density of states are expected to be more easily detectable than in double-well systems. The cyclotron mass, proportional to the density of states and characterizing the electron motion in tilted magnetic fields, is calculated as a function of in-plane magnetic field. The separability of the energy spectra resulting in tilted cyclotron orbits is demonstrated on the basis of a classical picture of an electron moving in crossed electric and magnetic fields.

1. Introduction

The electronic structure of bilayer 2D electron systems in double quantum wells has become a focus of interest since their preparation has been achieved, and intensive theoretical and experimental investigation of the properties of these systems is now in progress. The main directions of recent research on these structures subjected to magnetic fields were reviewed by Eisenstein [1]. Firstly, in a strong perpendicular magnetic field, the double-layer systems exhibit new quantum Hall states not present in a standard 2D gas because of an extra degree of freedom, the layer index. Secondly, in the in-plane magnetic fields, the tunnelling between two electron layers can be modified to such an extent that, at certain critical fields, the interlayer tunnelling is completely suppressed and electrons move exclusively in one of the wells. The field-induced decoupling of electron layers is accompanied by a number of new phenomena which can be studied by measuring both the parallel and perpendicular transport and the Shubnikov–de Haas effect.

A typical double-well structure consists of a pair of narrow ($\approx$20 nm) wells separated by an undoped AlGaAs barrier of a similar thickness. Two Si-doping layers are usually located both below and above the wells and the Schottky gates are deposited on the top/back of the sample to control better the concentration of electrons in individual wells. Due to the tunnelling through the barrier the degeneracy of the energy spectrum in the layer index is removed, the corresponding single levels split and the lowest bound states of individual

0953-8984/95/193721+12$19.50

wells form a symmetric/antisymmetric pair. A small tunnelling probability through the hard-wall AlGaAs barrier implies a small level splitting and a weak coupling of electron layers.

Traditionally, the gross features of the electronic structure of a standard double well are explained in terms of a simple model which assumes two identical very narrow wells at the distance d and a weak overlap of the localized states corresponding to first subbands of both wells. The interwell tunnelling is described in the tight-binding approximation by a single parameter determining a small bonding–antibonding energy gap. Then the band spectrum is given by the elementary nearly-free-electron model as presented in classical solid-state textbooks (see, e.g., [2]). The model predicts the anticrossing of two circular Fermi lines accompanied by the logarithmic van Hove singularity in the density of states which can be interpreted, in the 2D case, in terms of singular effective cyclotron mass. It was utilized to study the role of minigaps in Si by Ando [3] and Mathesson and Higgins [4] and successfully applied in the description of the interwell tunnelling (see [1] and references therein) and of the electronic structure of double wells in tilted magnetic fields [5–7].

In our theoretical study we shall consider another potentially bilayer system, the double-heterojunction quantum wells formed only by two selectively doped AlGaAs/GaAs interfaces with no AlGaAs layer grown between them. Note that in this case an undoped structure would result in an exactly rectangular quantum well. In the doped structures, the transfer of electrons from Si donors into the GaAs leads to band bending in the GaAs by electrostatic forces and, consequently, to the formation of a soft built-in barrier of approximately parabolic shape inside the well. Wether the built-in barrier is strong enough to separate the quantum well into two independent/weakly coupled parts or the coupling is so strong that the system can be considered as a transient form between a single well and a double well depends on the well width and the amount of charge. For simplicity, only symmetrically doped wells will be considered.

In charged wells, the shape of the barrier is given by the charge distribution. Therefore the electronic structure must be determined by the self-consistent solution of coupled Schrödinger and Poisson equations. A number of such calculations have been performed for the case of zero magnetic field—see, e.g., [8] and references therein. Effects of the in-plane magnetic field on both conduction and valence bands, resulting in a diamagnetic shift of the electron–hole recombination energy, were discussed by Oliveira *et al* [9], neglecting the exchange and correlation energies. Here the full self-consistent calculation will be employed to obtain the electron energy spectra and information about the charge redistribution due to the magnetic field. The electronic structure of double-heterojunction wells will be studied mainly from the point of view of the possible magnetic-field-induced splitting of a single-layer electron system to a bilayer one.

2. Band-structure calculation

The standard semi-empirical model, working quantitatively for the lowest conduction states of GaAs/AlGaAs heterostructures, is used to solve the Schrödinger equation in the envelope function approximation. The envelope function is assumed to be built up from host quantum states belonging to a single parabolic band. The effect of the effective-mass mismatch is completely neglected and the envelope functions of GaAs and AlGaAs are smoothly matched at the interface. Due to the translational invariance in the layer plane the momentum operators p_x and p_y become good quantum numbers, $p_x \rightarrow \hbar k_x$ and $p_y \rightarrow \hbar k_y$. If we choose a vector potential $\boldsymbol{A}$ in the form $\boldsymbol{A} = (B_y z, 0, 0)$, the eigenvalue problem reduces

to solving the one-dimensional Schrödinger equation with the Hamiltonian

$$H = \frac{1}{2m}p_z^2 + \frac{m\omega^2}{2}(z - z_0)^2 + V_{\text{conf}}(z). \tag{1}$$

(For a more detailed derivation, consistent with our notation, see, e.g., [10] and references therein.) The centre z_0 of the the magnetic part of the effective potential energy is related to the wave vector component k_x by $z_0 = \hbar k_x/m\omega$, where ω denotes the cyclotron frequency $\omega = |e|B_y/m$. The confining potential energy of a well with the width d

$$V_{\text{conf}}(z) = V_b(z) + V_{sc}(z) \tag{2}$$

is a sum of the step functions $V_b(z) = V_b\theta(-z - d/2) + V_b\theta(z - d/2)$, corresponding to the conduction band discontinuities between AlGaAs and GaAs, and of a term $V_{sc}(z)$ describing the interaction of an electron with ions and the electron–electron interaction. This term should be calculated self-consistently and can be written as

$$V_{sc}(z) = V_H(z) + V_{xc}(z). \tag{3}$$

The Hartree term V_H is the solution to the Poisson equation

$$\frac{d^2V_H}{dz^2} = \frac{|e|\varrho(z)}{\epsilon} \tag{4}$$

and we use an expression calculated by Ruden and Döhler [11] in a density-functional formalism for the exchange–correlation term V_{xc},

$$V_{xc} \simeq -0.611\frac{e^2}{4\pi\epsilon}\left(\frac{3N_e(z)}{4\pi}\right)^{1/3}. \tag{5}$$

The conduction band offset V_b and the dielectric constant ϵ enter our calculations as input parameters.

For modulation-doped GaAs/AlGaAs heterostructures the total charge density $\varrho(z)$ in equation (4) can be split into parts corresponding to concentrations of electrons, $N_e(z)$, their parent donors in AlGaAs, $N_d^+(z)$, and ionized residual acceptors in GaAs, $N_a^-(z)$,

$$\varrho(z) = e\left[N_e(z) - N_d^+(z) + N_a^-(z)\right]. \tag{6}$$

We accept the usual approximation of constant impurity concentrations and assume donors and acceptors to be ionized within certain finite intervals: $N_d^+(z) = N_d$ for $d/2 + w \leqslant |z| \leqslant d/2 + w + l_d$, i.e. symmetrically with respect to the well of width d, and $N_a^-(z) = N_a$ for $|z| \leqslant d/2$, which means that all acceptors inside the well are ionized. Here w denotes the spacer thickness and l_d is the depletion length of donors which is determined in the course of the self-consistent procedure.

3. Results and discussion

In our calculation we consider four wells with widths d = 25, 40, 50 and 60 nm, close to the dimensions of a typical double quantum well described above. The concentrations of localized charges are $N_d = 2 \times 10^{18}$ cm^{-3} and $N_a = 10^{14}$ cm^{-3}, the band offset $V_b = 225$ meV and the dielectric constant $\epsilon = 12.9$. The spacer thickness $w = 60$ nm yields electron systems with a concentration of electrons $N_e \approx 3.2 \times 10^{11}$ cm^{-2}. The self-consistent procedure was performed in two steps. Firstly, the electronic structure of wells was calculated in zero magnetic field, while in the second step the magnetic field dependence of subbands was obtained starting from intermediate zero-field results.

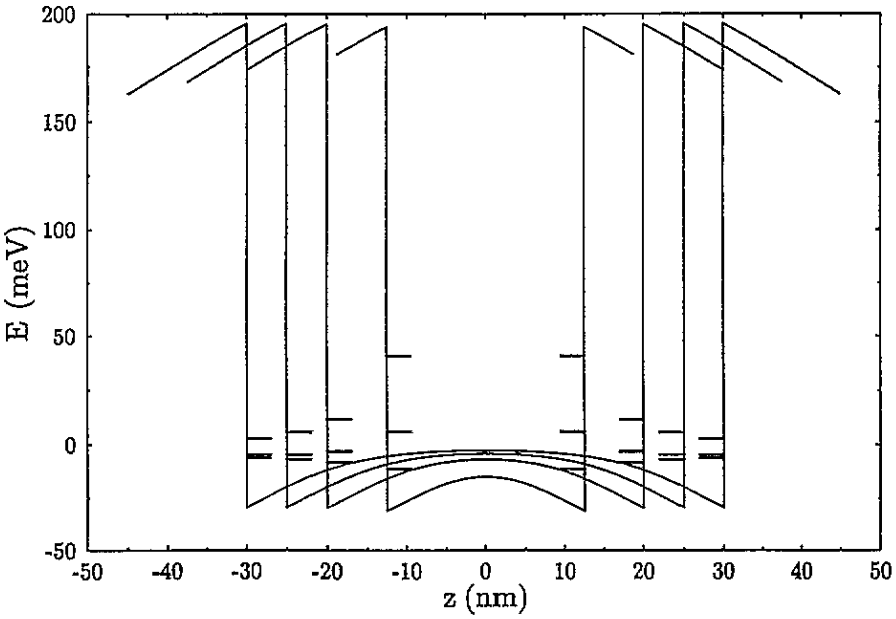

Figure 1. Band diagrams and energy levels of double-heterojunction wells in zero magnetic field.

3.1. Zero-magnetic-field case

It follows from the form of Hamiltonian (1) that, in the case of zero magnetic field, an electron motion in the z-direction is completely decoupled from the in-plane components. The energy spectrum consists of two quasi-continuous free-electron branches, the quadratic functions of the wave vector components k_x, k_y, and the energy levels corresponding to the bound states of a well. The positions of levels on the energy scale are presented in figure 1, together with the band diagrams resulting from the first step of the self-consistent procedure. The form of the barriers is approximately parabolic for all four wells; minor deviations from this shape may be observed for wider wells. The heights of barriers are very small when compared with hard walls of wells formed by the GaAs/AlGaAs interfaces. This indicates a stronger coupling between wells than in a standard double-well structure.

All the systems have one occupied pair of symmetric/antisymmetric subbands, except the 25 nm wide well where only the subband belonging to the lowest (bonding) state is occupied. Note that the origin of the energy scale in figure 1 is located at the Fermi energy E_F of the electron system. The energy spectrum of the 60 nm system corresponds to almost independent quantum wells; both occupied levels lie below the top of the barrier and the splitting of energy levels due to the quantum tunnelling is small. The coupling of 2D electron layers increases smoothly with the decreasing well width and the energy spectrum of the 25 nm well reminds one rather of a single well than of a double well since the energy difference between the bonding and the antibonding states is comparable with the difference between the energy of the first level and a bottom of the well.

The electron charge density $N_e(z)$ corresponds to well known behaviour of two coupled wells as described by a simple tight-binding model: there are two maxima of the density positioned symmetrically in each well, with the small but finite minimum at $z = 0$ for bonding states and $N_e(0) = 0$ for antibonding states. Of course, the maxima are closer and bonding state charge densities higher in narrower double wells.

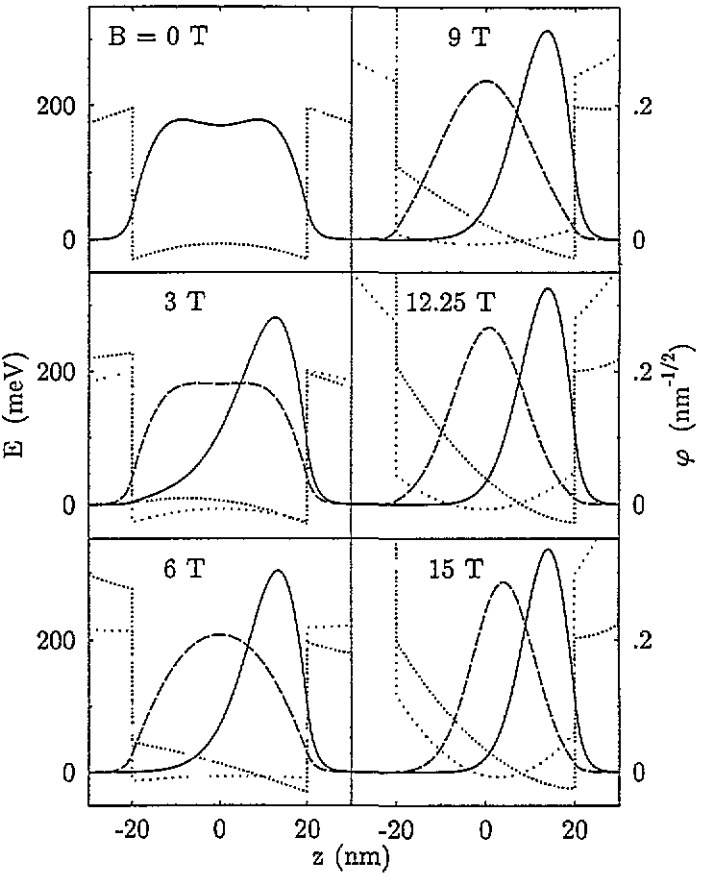

Figure 2. Wave functions and 'electromagnetic' band diagrams of a double-heterojunction well subject to in-plane magnetic fields. Pairs of curves characterize the electrons with a minimum (dashed) and a maximum (full) occupied $|k_x|$. The width of the well is 40 nm.

3.2. Magnetic-field-dependent band structure

As seen in figure 1, it is possible to approximate the form of barriers using an expression $-m\Omega^2 z^2/2$, where Ω is the fitting parameter. Assuming further that the barriers are not substantially changed by redistribution of electrons in the magnetic field, the potential energy in (1) is given by a combination of the fixed electric barrier and the attractive magnetic well with the curvature given by B_y. The position of the minimum, z_0, which need not lie inside the interval $-d/2, +d/2$, is determined by k_x. For small magnetic fields the potential energy inside the well is still a barrier with a smaller curvature $m(\omega^2 - \Omega^2)$ and a maximum at $z = z_0\,\omega^2/(\omega^2 - \Omega^2)$. At a critical magnetic field, $B_y = m\Omega/|e|$, the bottom of the well becomes a linear function of z, with the slope dependent on k_x, and at higher fields the sign of curvature of the potential energy line is reversed and a minimum appears at z instead of a maximum. The critical fields for the wells considered $B_{60} = 4.7$ T, $B_{50} = 5.6$ T, $B_{40} = 6.7$ T and $B_{25} = 9$ T, are fully in the range of experimentally available values. This distinguishes the double-heterojunction structures from the standard double wells with steep AlGaAs barriers in which two deep minima are preserved for arbitrary magnetic fields. Consequently, the simple tight-binding picture of

eigenfunctions as symmetric/antisymmetric combinations of the eigenstates of individual wells is no longer appropriate. Above a critical field the lowest eigenstates always exhibit a single maximum and thus electrons are more localized by the magnetic field around its centroid then in the case of standard structures. Examples of eigenfunctions together with 'electromagnetic' potential energy lines defined by equation (1) are presented in figure 2. The results are plotted for selected values of B_y and, to demonstrate their k_x-dependence, also for a minimum and a maximum $|k_x|$ corresponding to occupied states.

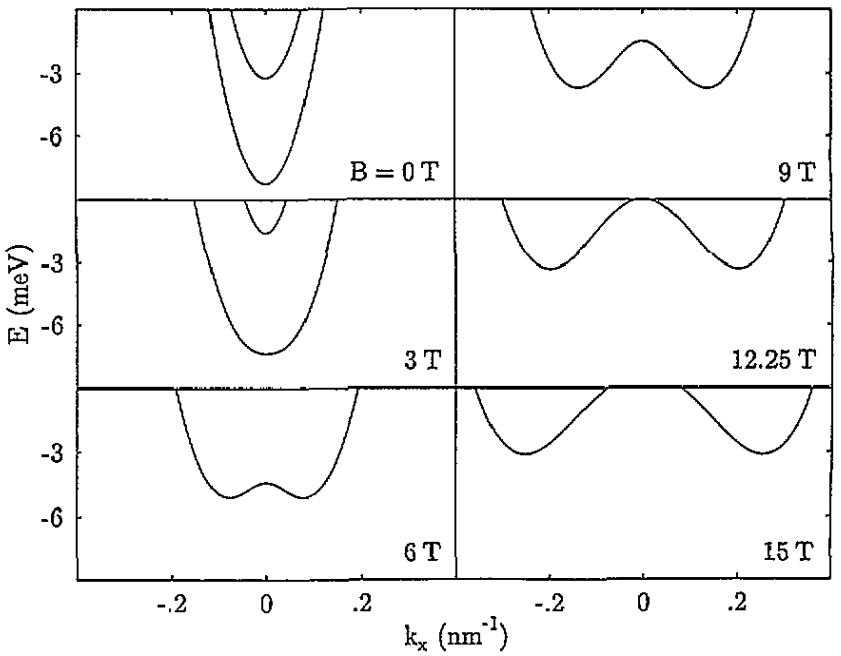

Figure 3. Occupied energy subbands of a double-heterojunction well, $d = 40$ nm, subject to in-plane magnetic fields as functions of k_x.

The transition from a single-layer to a bilayer electron system, induced by the in-plane magnetic field, is clearly visible in figure 2. Moreover, the effective interlayer separation increases with the magnetic field reaching a value equivalent to the width of the central GaAs region, in the strong-magnetic-field limit. These effects are absent in standard double-well systems where the distance between 2D electron layers is a constant given by the separation between wells.

It follows from the above discussion that the in-plane magnetic field does not influence the harmonic dependence of subbands on k_y at all, but the dependence on k_x is changed dramatically. Firstly, the energy separation of bottoms of the bonding/antibonding pair of subbands increases with growing B_y. This process is accompanied by the continuous transfer of electrons from the higher occupied subband to the lower one until the second subband is completely depleted. Secondly, the curvature of the originally parabolic subbands is modified. The antibonding subband remains almost parabolic, similarly to what is found in zero field, only its curvature is slightly higher for larger B_y. The bonding subband exhibits more varied field dependence. The curvature of $E(k_x)$ decreases for k_x around $k_x = 0$; at a certain value of k_x it reaches zero and then becomes negative. This means that, instead of a minimum which corresponds to zero field, the local maximum develops at $k_x = 0$ accompanied by two new minima positioned symmetrically around it. For large enough

magnetic fields the energy of the maximum becomes greater than the Fermi energy and the spectrum of occupied energies splits into two separated parts. This type of behaviour is general for energy spectra of all four well widths. In the narrowest well the splitting does not occur in the range of fields investigated. Examples of $E(k_x)$ curves for the well of medium width, d = 40 nm, and several selected values of B_y are presented in figure 3.

The electrons with energies close to the Fermi energy E_F are of particular interest since they play an essential role in the electronic transport properties of the system. The occupied and empty states are separated by the Fermi lines in k-space. In a zero magnetic field, the Fermi contours corresponding to symmetric and antisymmetric subbands take the form of two concentric circles. The larger circle describes the bonding and the smaller circle the antibonding states. The modification of the shape of $E(k_x)$-curves by the in-plane magnetic fields is reflected also in variation of the forms of the Fermi contours. They acquire 'peanut' and a 'lens' shapes when the sample is subjected to the intermediate magnetic fields. In the strong-field limit the 'lens' is emptied and the 'peanut' is split into two parts belonging to individual wells. This behaviour is illustrated in figure 4 for the same electron system and the same set of magnetic field values as in figure 3. The deviations from two crossing circles, corresponding to a pair of narrow independent wells, are so large that the shape of the Fermi lines can hardly be described by the above-mentioned simple model.

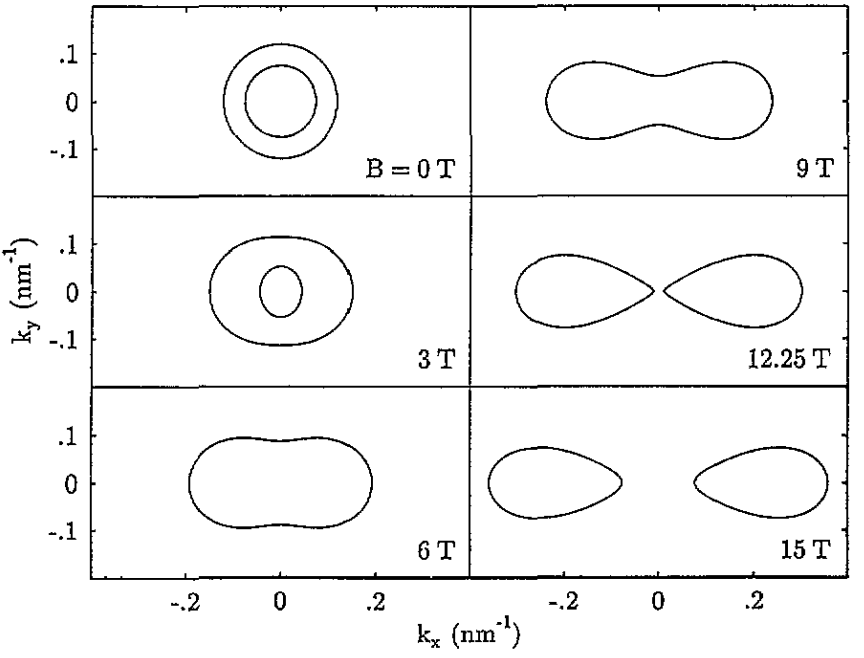

Figure 4. Fermi contours of a double-heterojunction well, d = 40 nm, subject to in-plane magnetic fields.

3.3. Cyclotron effective mass and real-space trajectories

The separation of electron layers by the in-plane magnetic field may be clearly demonstrated if we consider the electronic structure of a system subjected to a tilted magnetic field with a strong component B_y, parallel to the GaAs/AlGaAs interfaces, and a weak component B_z oriented perpendicularly. To describe the system, the self-consistent quantum mechanical

calculation of the electron subbands in the presence of B_y, presented above, is combined with a quasi-classical description of the in-plane electron motion under the influence of B_z, as developed originally by Onsager [12] and Lifshitz [13].

The semiclassical theory predicts that an electron is driven by the Lorentz force due to B_z around the Fermi contour with the cyclotron frequency $\omega_c = |e|B_z/m_c$. The cyclotron effective mass m_c, defined by the above equation, is an important characteristic of each Fermi line as a whole and should not be confused with the electron effective mass which is in our case a tensor and an anisotropic function of the position on the Fermi line. The explicit expression relating m_c to the shape of the Fermi contour is

$$m_c = \frac{\hbar^2}{2\pi} \oint \frac{dk}{|\nabla_k E|} \tag{7}$$

where dk denotes an element of a length of a Fermi line. In the case of two-dimensional electron systems a simple relation holds between the cyclotron effective mass and the density of states g corresponding to a single subband:

$$g = \frac{m_c}{\pi\hbar^2}. \tag{8}$$

Note that this is the cyclotron effective mass, and not the effective mass, which determines, for example, the temperature damping of Shubnikov–de Haas oscillations.

Equations (7) and (8) can already both be found, at least in an implicit form, in [12] and [13]. Since they were obtained they have been utilized many times (for applications to 2D systems see, e.g., [4]), but they were overlooked in the recent publication by Harff *et al* [14]. Their detailed derivation and discussion for the case of combined parallel and perpendicular magnetic fields is presented in [10].

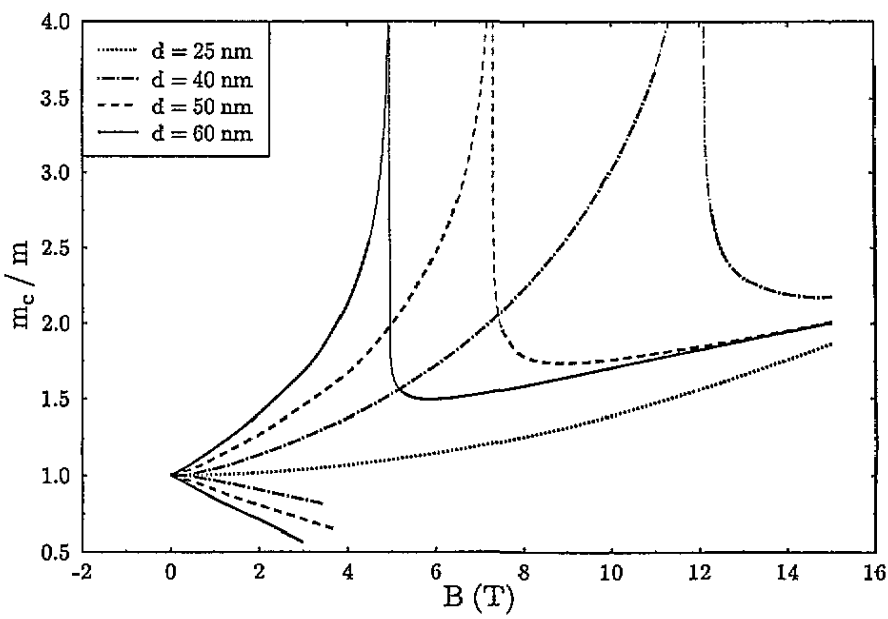

Figure 5. Cyclotron effective masses of four wells as functions of an in-plane magnetic field.

The magnetic-field-dependent cyclotron effective masses resulting from our band-structure calculation are shown in figure 5 for all four wells. The logarithmic singularities

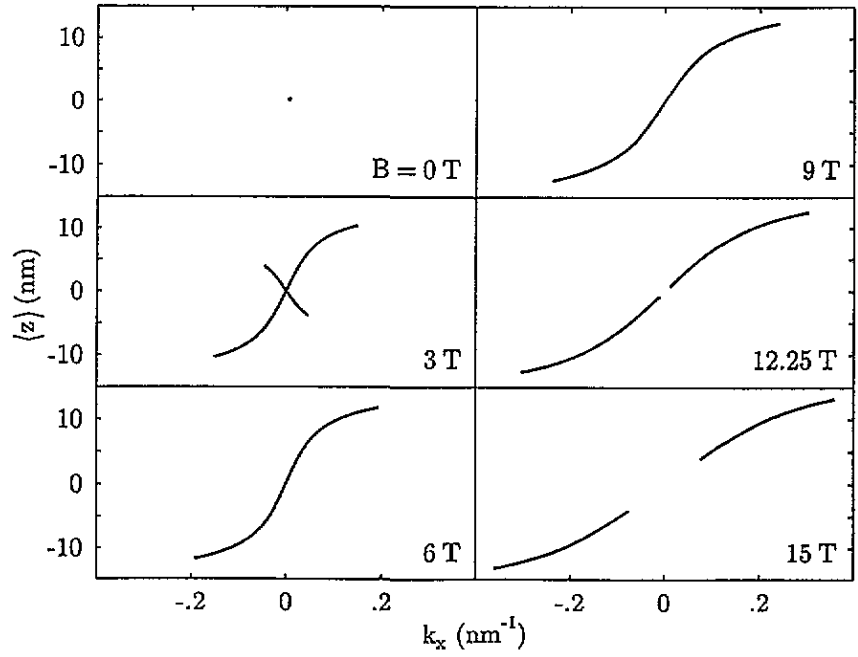

Figure 6. Centroids of electron states of a double-heterojunction well, $d = 40$ nm, subject to in-plane magnetic fields.

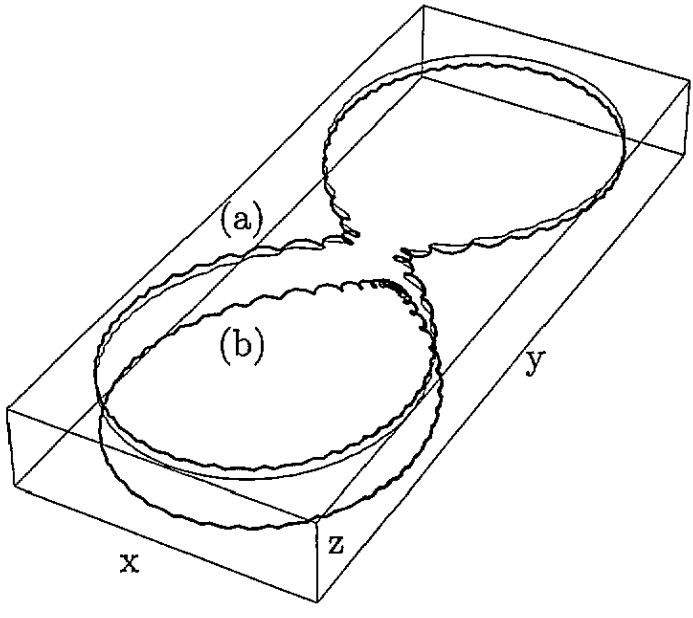

Figure 7. Classically calculated trajectories of an electron in a double well subject to a tilted magnetic field. The upper curve (a) corresponds to B_y below the singularity and the lower curve (b) to B_y above this value.

of the cyclotron mass (density-of-states) curves corresponding to the lowest subbands occur at higher fields for narrower wells than for broader ones. The position of a singularity is

identical with the field value at which a 'peanut' becomes a pair of 'kissing' Fermi contours, i.e. when it is to split into two independent parts. Note that this is always above the fields $B_{60} = 4.7$ T, $B_{50} = 5.6$ T and $B_{40} = 6.7$ T discussed above. The asymmetric shape of van Hove singularities somewhat deviates from the expression $-\ln|E_F(B_y) - E_0|$ predicted by the analysis based on the quadratic approximation of the energy spectrum near the saddle point. The reason for the slow increase of m_c on the left of the singularity, and the rapid decrease on the right, may be due to the large influence of higher-order terms in the power expansion of $E(k_x)$. For the Fermi contours of the second subband the cyclotron mass always decreases for the given concentration of electrons.

In the real space, electrons move along trajectories having the shape of Fermi contours but rotated by an angle $\pi/2$ and multiplied by $\hbar/|e|B_z$. A relation exists between the centre of mass $\langle z \rangle$ of an electron state in a well and the energy spectrum $E(k_x)$ modified by the in-plane magnetic field,

$$\langle z \rangle = \frac{\hbar k_x}{m\omega} - \frac{1}{\hbar\omega}\frac{\partial E(k_x)}{\partial k_x}. \tag{9}$$

Since $\langle z \rangle$ is a function of k_x, i.e. of the position of an electron on the Fermi contour, the real-space trajectory is slightly tilted with respect to the x–y-plane. Travelling around a 'peanut' Fermi contour with the frequency ω_c, the electron is transmitted from one well to the other when the wavevector k_x changes its sign. At $k_x = 0$ the electron appears on the top of the barrier. The separation of a 'peanut' into two parts means that two independent real-space trajectories for electrons are formed, localized completely in opposite wells. In that case, the electron moving around a Fermi contour is always reflected by the barrier and remains confined in one of the wells. Hence, the electron system can be considered as divided into two disconnected layers. Self-consistently calculated examples of $\langle z \rangle$ as a function of k_x are presented in figure 6.

The quasi-classical model of an electron motion in a double well can help to illustrate the origin of localization of electrons in individual wells due to the magnetic field. Figure 7 shows real-space trajectories of an electron in a well with a parabolic barrier calculated classically for the case of two tilted magnetic fields with the same perpendicular component. For the field below the singularity, the trajectory overcomes the barrier and an electron spends the same time in both wells. Note that, in accordance with this statement, the left-hand part of the curve (a) lies above and the right-hand part below the projection of the trajectory to the x–y-plane ($z = 0$). The curve (b) is the electron trajectory calculated for the field above the singularity (the curves (a) and (b) are offset for clarity). In that case, an electron is kept in one well all the time. Just at the magnetic field where the singularity occurs, the electron stops at the top of the barrier and stays there infinitely. This means, in the terms utilized above, that its cyclotron frequency is zero and the cyclotron mass goes to infinity.

4. Conclusion

We have performed self-consistent calculations on the electronic structure of symmetrically charged double-heterojunction wells in parallel magnetic fields. The properties are found to be to a large extent similar to those of standard double wells but, on the other hand, there are several differences that make the double heterojunctions attractive.

In both types of structure an in-plane magnetic field substantially modifies the k_x-dependence of the energy subbands. The following properties result from these field-induced changes. (i) Electrons are transferred from the antibonding to the bonding band when the

magnetic field increases. (ii) The Fermi contour topology changes—the originally circular lines acquire a 'peanut' and a 'lens' shapes and, at certain critical fields, the 'lens' is emptied (*first critical field*) and the 'peanut' splits into two independent lines (*second critical field*). (iii) The splitting of the 'peanut' Fermi contour is accompanied by the separation of an electron layer into two independent systems. (iv) At the second critical field the density of electron states and the cyclotron effective mass exhibit a logarithmic singularity when considered as functions of the in-plane field.

The forming of a hard-wall barrier by the AlGaAs layer means that the coupling between electrons in a standard double well is always weak. Therefore, a simple tight-binding method for description of electron motion in the z-direction, resulting in a nearly-free-electron model for its motion in the x–y-plane, can be successfully applied to describe the electronic structure.

This is not true for double-heterojunction systems. Due to the charge present inside wells, a soft barrier of approximately parabolic shape is built in each well, with the top at its centre. The height of the barrier is very small and the strength of coupling can be tuned over a large range by proper choice of the concentration of carriers and the width of the well. Under these circumstances, the simple model fails to describe the electronic spectra even in a qualitative way. Note that according to our calculations, the gap between two occupied subbands, for example, increases under the influence of the field, while the simple model yields a constant gap.

The strong coupling between wells means that stronger magnetic fields are necessary to modify the electronic structure of a double heterojunction. The difference between the first and second critical fields can amount several tesla and, consequently, the changes of the cyclotron effective mass are also more robust and probably easier to detect experimentally.

Nevertheless, the above-described differences between two types of structure are mainly quantitative. The qualitatively new features of double-heterojunction structures are the single-layer/bilayer transition and the possible control of the interlayer separation using the in-plane magnetic field. These effects might be useful in studies of many-body effects in bilayer electron systems.

Because of these properties the double-heterojunction structures represent a very attractive alternative to standard double wells.

Acknowledgments

This was supported by the Grant Agency of the Czech Republic under Grant No 202/94/1278, by the Ministry of Education, Czech Republic, under contract No V091, and by NSF, US, through the grant NSF INT-9106888.

References

[1] Eisenstein J P 1992 *Superlatt. Microstruct.* **12** 107
[2] Mott N F and Jones H 1936 *The Theory of the Properties of Metals and Alloys* (London: Oxford University Press) p 59
[3] Ando T 1979 *J. Phys. Soc. Japan* **47** 1595
[4] Matheson T G and Higgins R J 1982 *Phys. Rev.* B **25** 2633
[5] Hu J and MacDonald A H 1992 *Phys. Rev.* B **46** 12 554
[6] Lyo S K 1994 *Phys. Rev.* B **50** 4965
[7] Kurobe A, Gastleton I M, Linfield E H, Grimshaw M P, Brown K M, Ritchie D A, Pepper M and Jones G A C 1994 *Phys. Rev.* B **50** 4889
[8] Simserides C D and Triberis G P 1993 *J. Phys.: Condens. Matter* **5** 6437

[9] Oliveira G M G, Gomes V M S, Chaves A S, Leite J R and Worlock J M 1987 *Phys. Rev.* B **35** 2896
[10] Smrčka L and Jungwirth T 1994 *J. Phys.: Condens. Matter* **6** 55
[11] Ruden P and Döhler G H 1983 *Phys. Rev.* B **27** 3538
[12] Onsager L 1952 *Phil. Mag.* **43** 1006
[13] Lifshitz I M 1956 *Sov. Phys.–JETP* **30** 63
[14] Harff N E, Simmons J A, Lyo S K, Klem J F and Goodnick S M 1995 *ICPS-22 Proc.* at press